6. J. T. Snow, *Rev. Geophys Space Phys.* **20**, 953 (1982).
7. E. A. Rasmussen *et al.*, *Bull. Am. Meteorol. Soc.* **75** 995 (1994).
8. H. B. Bluestein and J. H. Golden, in *The Tornado: Its Structure, Dynamics, Prediction and Hazards* (*Geophys. Monogr. Am. Geophys. Union* **79**, American Geophysical Union, Washington, DC, 1993), pp. 319–352.
9. H. B. Bluestein, J. G. LaDue, H. Stein, D. Speeder, W. P. Unruh, *Mon. Weather Rev.* **121**, 2200 (1993).
10. J. Wurman, J. M. Straka, E. N. Rasmussen, M. Randall, A. Zahrai, preprint, 27th American Meteorlogical Society International Conference on Radar Meteorology, Aspen, CO, 1995.
11. ———, in preparation.
12. We made scans at elevation angles of 0°, 1°, 2°, 4°, 6°, 8°, 10°, 12°, 14°, and 18° elevation, every 95 s, with a scan rate of 10° s^{-1}, using 64 pulses per beam and a Nyquist interval of 32 $m\ s^{-1}$. Plotted radar times were 2 min ahead of UTC.
13. The Doppler velocity data contained folds at ±16 and ±48 $m\ s^{-1}$, which were manually unfolded to produce the velocity fields shown in the figures.
14. R. J. Doviak and D. S. Zrnic', *Doppler Radar and Weather Observations* (Academic Press, New York, 1993).
15. Small-scale suction vortices, 10 to 30 m in diameter, were not unambiguously revealed in either the 50- to 75-m radar resolution volumes of reflectivity or in velocity data retrieved at Dimmitt, TX. It is possible that higher velocities exist in these features, although this was not indicated by the damage survey. Very few structures were struck and therefore damaged by this tornado.
16. We used the following software packages to analyze the data and produce the figures: Solo (to display and unfold raw data); Reorder (to interpolate to Cartesian grids); and Zebra (to display gridded data), developed by the Research Data Program of the Atmospheric Technology Division at the National Center for Atmospheric Research (NCAR).
17. An advective correction of 6.2 $m\ s^{-1}$ from 185° (from just west of south) was applied to correct for the time skew between low- and high-altitude observations. The grid spacing was 50 m. The nearest-neighbor method was used to interpolate to the Cartesian grid.
18. Supported by the University of Oklahoma (J.M.S. and J.W.); the National Oceanic and Atmospheric Administration, National Severe Storms Laboratory (NSSL) (E.N.R., J.M.S., and J.W.); NCAR, Atmospheric Technology Division, Remote Sensing Facility (J.W.); and the Center for the Analysis and Prediction of Storms through NSF grant ATM-912 0009 (J.M.S. and J.W.). The Cooperative Institute for Mesoscale Meteorological Studies, at the University of Oklahoma, also played an important role. The truck for the mobile radar was provided by NSSL (R. Maddox and D. Forsythe), and the radar transmitter was provided by NCAR (D. Carlson and P. Hildebrand). M. Randall and E. Loew provided the software and hardware for the PC Integrated Radar Acquisition data acquisition system. A. Zahari designed the antenna controller. D. Nealson and P. Griffin provided assistance in building and maintaining the radar. L. Chan prepared this manuscript.

12 February 1996; accepted 3 May 1996

Ion-Induced Morphological Changes in "Crew-Cut" Aggregates of Amphiphilic Block Copolymers

Lifeng Zhang, Kui Yu, Adi Eisenberg*

The addition of ions in micromolar ($CaCl_2$ or HCl) or millimolar (NaCl) concentrations can change the morphology of "crew-cut" aggregates of amphiphilic block copolymers in dilute solutions. In addition to spherical, rodlike, and univesicular or lamellar aggregates, an unusual large compound vesicle morphology can be obtained from a single block copolymer. Some features of the spontaneously formed large compound vesicles may make them especially useful as vehicles for delivering drugs and as models of biological cells. Gelation of a dilute spherical micelle solution can also be induced by ions as the result of the formation of a cross-linked "pearl necklace" morphology.

Most aggregates formed by the self-assembly of amphiphilic block copolymers in selective solvents are spherical and consist of a core and a coronal shell. The core is composed of the insoluble blocks, whereas the corona contains the soluble blocks, which are highly swollen by the solvent. Such structures have been explored in detail (*1*). We have described the formation of aggregates of multiple morphologies of one family of highly asymmetric polystyrene-*b*-poly(acrylic acid) (PS-*b*-PAA) in dilute solution (*2*) in which the length of the insoluble PS blocks was much longer than that of the soluble PAA blocks. They were therefore described as "crew-cut" aggregates. As the length of the PAA block decreased, the morphology of the aggregate changed from spherical to rodlike, to lamellar or vesicular, and finally to large compound micelles (LCMs) consisting of an assembly of inverted spherical micelles surrounded by a hydrophilic surface. A more detailed description of the multiple morphologies and the characteristics of the crew-cut micellelike aggregates is available (*3*). More recently, it was shown that PS-*b*-poly(ethylene oxide) (PS-*b*-PEO) diblocks in dilute solution can also form aggregates with various morphologies from block copolymers of different compositions (*4*).

Morphological changes can also be induced in an identical block copolymer by the addition of ions in micromolar ($CaCl_2$ or HCl) or millimolar (NaCl) concentrations. The morphologies are the same as those produced by changes in the copolymer composition in the absence of added ions, which suggests that the morphological changes are probably induced by decreased repulsion (both steric and electrostatic) among the hydrophilic segments as a result of protonation of PAA (by HCl) or of ion binding or bridging (by Ca^{2+}). In addition, aggregates of a new morphology, consisting of large compound vesicles (LCVs), were prepared and are described. The LCVs may be useful as possible drug-delivering vehicles and as models of stable microstructured biomaterials. Finally, ion-induced gelation can occur in which spherical micelles in aqueous solution form a cross-linked "pearl necklace" structure in the presence of 20 mM HCl. These results suggest that the versatility of the crew-cut aggregates is much greater than originally suspected.

The PS-*b*-PAA or PS-*b*-PEO diblocks were dissolved in *N*,*N*-dimethylformamide (DMF) to give a stock solution of 1 weight %. Deionized water was then added to the copolymer solutions with stirring; micellization took place between about 4 and 6 weight % of water. However, the addition of water was continued until the solution was 25 weight % of water to ensure that the structure of the formed aggregates was kinetically frozen. We isolated the aggregates into water by dialyzing the resulting solutions against distilled water to remove the DMF. A dynamic equilibrium between aggregates and unimers undoubtedly exists in the early stages of water addition during micellization. At some point, however, as the DMF is forced out of the core, the equilibrium is frozen because of the glassy nature of the PS chains.

Table 1. Summary of the effect of added acid or salt concentration (with *R* given in parentheses) on the aggregate morphology of a PS(410)-*b*-PAA(25) diblock copolymer.

Acid or salt concentration (M) and *R*	Dominant morphology
HCl	
1.9×10^{-4} (0.035)	Spheres
2.1×10^{-4} (0.040)	Rods
2.4×10^{-4} (0.045)	Vesicles
2.7×10^{-4} (0.050)	LCVs
NaCl	
2.1×10^{-3} (0.40)	Spheres
3.2×10^{-3} (0.60)	Rods
1.1×10^{-2} (2.0)	Vesicles
2.1×10^{-2} (4.0)	LCVs
$CaCl_2$	
1.2×10^{-4} (0.023)	Spheres
1.4×10^{-4} (0.026)	Vesicles
2.8×10^{-4} (0.053)	LCVs

Department of Chemistry, McGill University, 801 Sherbrooke Street West, Montreal, Quebec, Canada H3A-2K6.

*To whom correspondence should be addressed.

A set of transmission electron microscopy (TEM) images (5) of the aggregates prepared from the same diblock copolymer [PS(410)-*b*-PAA(25); the numbers in parentheses indicate the degree of polymerization of the blocks] at different concentrations of added HCl is shown (Fig. 1). Without added acid, the aggregates were small spheres of low polydispersity with an average diameter of 29 nm. When the HCl concentration was 190 μM (or a molar ratio *R* of added HCl to acrylic acid repeat units of 0.035), the aggregates were still spherical (Fig. 1A) but with an average diameter of 38 nm. However, for 210 μM HCl (*R* = 0.040), spherical, rodlike, vesicular, and lamellar aggregates coexisted in the solution (Fig. 1B), the predominant morphology being rodlike. For 240 μM HCl (*R* = 0.045), most of the aggregates became vesicular, with rodlike aggregates observed occasionally (Fig. 1C); for 270 μM HCl (*R* = 0.050), the aggregates became LCVs (Fig. 1D). The same morphology was observed for 530 μM HCl (*R* = 0.10); no further morphological change was observed. Addition of salt can also induce morphological changes of the aggregates. The effect of divalent ions, such as Ca^{2+}, was much stronger than that of univalent ions, such as Na^+ (Table 1).

The usefulness of ions in controlling block copolymer morphology was also demonstrated when HCl was added to spherical micelles of PS(500)-*b*-PAA(60) in pure water, in which the PS cores were below their glass transition temperature. When HCl was added to a 1 weight % aqueous solution of the spherical copolymer aggregates to an acid content of ~20 mM (*R* = 2), the solution gelled over a very narrow range of acid content. Electron microscopy showed that a pearl necklace morphology was formed, with occasional multifunctional beads maintaining the gelled network (Fig. 2). The pearl necklace morphology was most likely a result of the acid driving the spheres to form rods. However, the glassy nature of the PS cores of the beads made it impossible to complete the transformation. The pearl necklace thus represents an intermediate step between spheres and rods.

Ion-induced morphological changes were also found in PS-*b*-PEO. For example, PS(240)-*b*-PEO(80) gave rods in the absence of salt but gave lamellae and vesicles in the presence of 1.3 mM LiCl (*R* = 0.10) (Fig. 3). Preliminary results suggest that the PS-*b*-poly(4-vinylpyridinium methyl iodide) (PS-*b*-P4VP.MeI) also yields multiple morphologies in the presence of salt (6). The P4VP.MeI is ionic, PAA is ionizable, and PEO is nonionic. Thus, the control of aggregate morphology of amphiphilic block copolymers by micromolar concentrations of ions seems to be general.

The LCVs appear to be a new morphology. They were also observed for PS(410)-*b*-PAA(13) with 255 μM HCl (*R* = 0.09) (Fig. 4A), for PS(240)-*b*-PEO(15) without

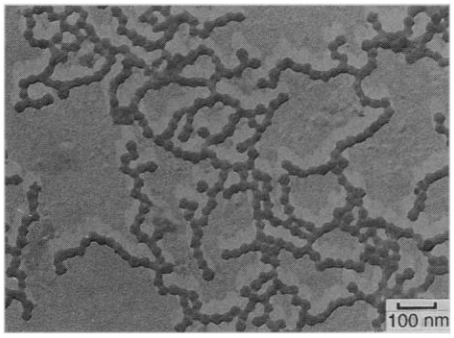

Fig. 2. Pearl necklace morphology of the aggregates in the gelled aqueous solution of spherical micelles of PS(500)-*b*-PAA(60) that was induced by the addition of HCl (~20 mM). Sonication was used to break down the gel network structure for TEM sample preparation.

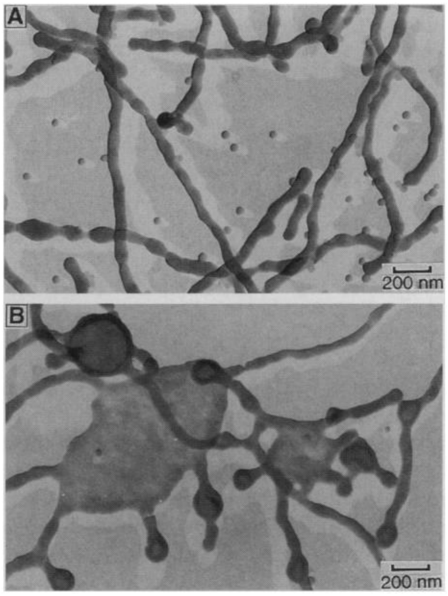

Fig. 3. Aggregates made from PS(240)-*b*-PEO(80) (**A**) in the absence of salt and (**B**) in the presence of 1.3 mM LiCl (*R* = 0.10).

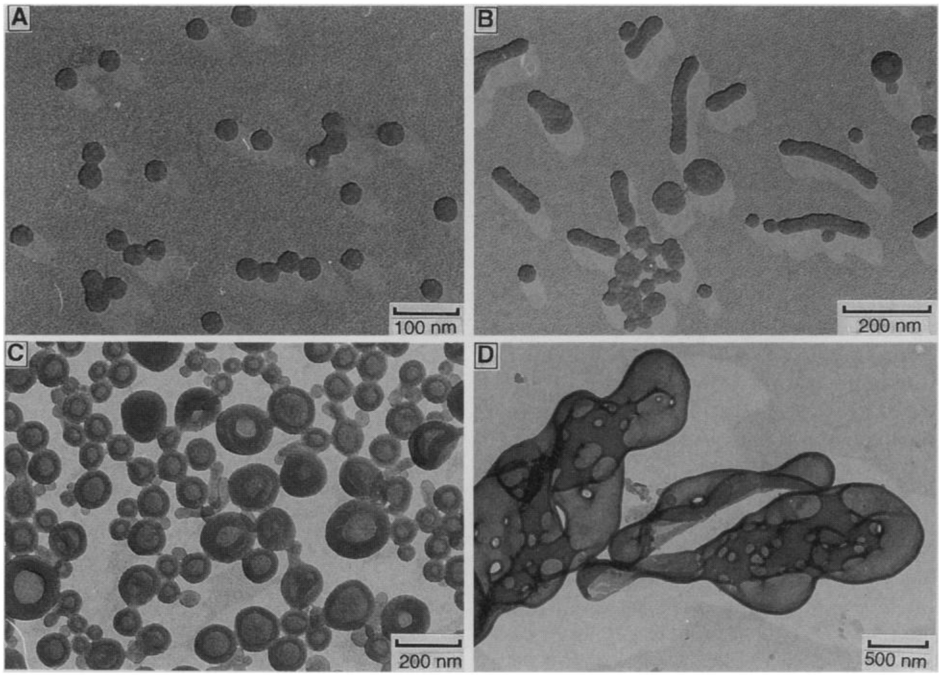

Fig. 1. Aggregates of various morphologies made from PS(410)-*b*-PAA(25) by the addition of HCl to the following different final concentrations: (**A**) 190 μM (*R* = 0.035), (**B**) 210 μM (*R* = 0.040), (**C**) 240 μM (*R* = 0.045), and (**D**) 270 μM (*R* = 0.050).

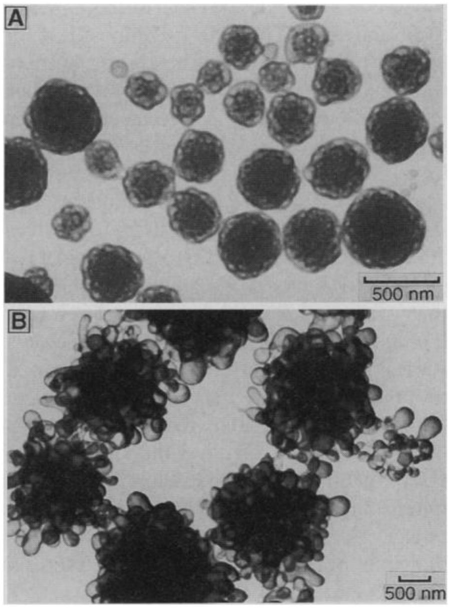

Fig. 4. LCVs made from (**A**) PS(410)-*b*-PAA(13) in the presence of 255 μM HCl (*R* = 0.09) and from (**B**) PS(240)-*b*-PEO(15) in the absence of salt.

any added salt (Fig. 4B), and for PS(240)-*b*-PEO(45) with 1.6 mM KF ($R = 0.10$). In the PS-*b*-PAA system, the thicknesses of both the inside and outside walls of the aggregates are uniform and equal. Their structure bears some resemblance to that of aggregated soap bubbles, and their outer surface must be hydrophilic because of the presence of the short PAA chains. The LCVs are irregular in shape in Fig. 1D but are more nearly spherical in Fig. 4. These differences may be due to the polydispersity of the primary vesicles and the softness of the wall, as well as the surface energy and the shear conditions under which the LCVs were formed. The LCVs are subject to settling due to gravity but are stable and do not coalesce at room temperature. They can also be resuspended after settling. This aggregation process may provide an easy way to trap chemicals or drugs and then isolate them from the solution.

The self-assembly of vesicles has become a topic of current interest (*7*). Chemical species (that is, bisphospholipids) were incorporated into the vesicle walls to aid aggregation of these species into higher order (multivesicular) structures. As shown here, LCVs can be formed spontaneously under various conditions. They are thus a normal aggregate morphology. These higher order structures might be of interest in the development of methods for processing artificial tissuelike composites and soft biomaterials (*7*). In addition, the application of these structures in controlled drug delivery is a distinct possibility because the multiple concentric layers could provide a convenient timing mechanism.

The aggregate morphology of small-molecule amphiphiles can be changed by added salt (*8*), but much higher salt concentrations are needed (usually $\geq 10^{-1}$ M) compared with those in the present system (10^{-4} M for $CaCl_2$ or 10^{-2} M for NaCl). Changing the salt or acid content has a parallel effect on the morphology, as does changing the copolymer composition (*2*, *3*). Thus, the morphological changes appear to be a result of a gradual decrease in repulsion among the corona chains as the concentration of added ions increases. Both steric and electrostatic repulsions are involved among the partially ionized PAA chains (*9*). The addition of the strong acid, HCl, protonates the ionized carboxylic acid groups and shifts the PAA to a lower degree of ionization; as a result, the overall repulsion among the PAA chains is decreased.

At the onset of the morphological transition from spheres to vesicles for PS(410)-*b*-PAA(25), the $CaCl_2$ concentration is equivalent to 2.3 Ca^{2+} per 100 acrylic acid repeat units; thus, two PAA blocks share one Ca^{2+} if all the added Ca^{2+} is near the PAA chains. When the aggregates are LCVs, the number of Ca^{2+} ions per PAA block is about 1.5. Thus, the morphogenic effect is believed to be due to Ca^{2+} binding to the carboxylic acid of the PAA. Both inter- and intramolecular bridging appears possible. As a result, the effective distance between the PAA blocks is greatly reduced, which has the same effect on the morphology as does a decrease in block length. The relatively weaker morphogenic effect of added NaCl can be ascribed to both weak Na^+ binding and a screened electrostatic field of the charged PAA segments. The morphological changes in PS-*b*-PEO are also most likely caused by ion binding to the PEO blocks.

REFERENCES AND NOTES

1. C. Price, in *Developments in Block Copolymers*, I. Goodman, Ed. (Applied Science, London, 1982), vol. 1, pp. 39–80; J. Selb and Y. Gallot, *ibid.*, I. Goodman, Ed. (Applied Science, London, 1985), vol. 2, pp. 27–96; Z. Tuzar and P. Kratochvil, in *Surface and Colloid Science*, E. Matijevic, Ed. (Plenum, New York, 1993), vol. 15, pp. 1–83; M. D. Whitmore and J. Noolandi, *Macromolecules* **18**, 657 (1985); A. Halperin, *ibid.* **20**, 2943 (1987); R. Nagarajan and K. Ganesh, *J. Chem. Phys.* **90**, 5843 (1989); R. Hilfiker, D. Q. Wu, B. Chu, *J. Colloid Interface Sci.* **135**, 573 (1990); A. P. Gast, P. K. Vinson, K. A. Cogan-Farinas, *Macromolecules* **26**, 1774 (1993); I. Astafieva, X. F. Zhong, A. Eisenberg, *ibid.*, p. 7339; A. Qin, M. Tian, C. Ramireddy, S. E. Webber, P. Munk, *ibid.* **27**, 120 (1994); M. Antonietti, S. Heinz, M. Schmidt, C. Rosenauer, *ibid.*, p. 3276; O. Glatter, G. Scherf, K. Schillén, W. Brown, *ibid.*, p. 6046; L. Zhang, R. J. Barlow, A. Eisenberg, *ibid.* **28**, 6055 (1995).
2. L. Zhang and A. Eisenberg, *Science* **268**, 1728 (1995).
3. ______, *J. Am. Chem. Soc.* **118**, 3168 (1996).
4. K. Yu and A. Eisenberg, unpublished results.
5. A. Phillips EM410 microscope was used for the TEM studies. Samples were deposited from aqueous solutions onto copper EM grids that had been precoated with a thin film of polyvinyl formaldehyde plastic (Formvar) and then coated with carbon; the grids were then shadowed with a palladium-platinum alloy. A detailed description of the experimental conditions can be found elsewhere (*3*).
6. H. Shen and A. Eisenberg, unpublished results.
7. S. Chiruvolu *et al.*, *Science* **264**, 1753 (1994).
8. S. Ozeki and S. Ikeda, *J. Colloid Interface Sci.* **87**, 424 (1982); Y. Talmon, D. F. Evans, B. W. Ninham, *Science* **221**, 1047 (1983); D. D. Miller, D. F. Evans, G. G. Warr, J. R. Belare, B. W. Ninham, *J. Colloid Interface Sci.* **116**, 598 (1987); F. J. Schepers, W. K. Toet, J. C. van de Pas, *Langmuir* **9**, 956 (1993); B. J. Ravoo and J.B.F.N. Engberts, *ibid.* **10**, 1735 (1994); A. Sein and J.B.F.N. Engberts, *ibid.* **11**, 455 (1995); S. Miyagishi, H. Kurimoto, T. Asakawa, *ibid.*, p. 2951; L. L. Brasher, K. L. Herrington, E. W. Kaler, *ibid.*, p. 4267.
9. L. Zhang and A. Eisenberg, unpublished results.
10. We thank H. Shen for his consent to report results of preliminary experiments with the PS-*b*-P4VP.MeI system and C. J. Clarke, M. Moffitt, and L. Cuccia for useful discussions. We also thank the Natural Science and Engineering Research Council of Canada (NSERC) for continuing support of this research.

6 March 1996; accepted 25 April 1996

Patch-Clamp Detection of Neurotransmitters in Capillary Electrophoresis

Owe Orwar, Kent Jardemark, Ingemar Jacobson,*
Alexander Moscho, Harvey A. Fishman, Richard H. Scheller,
Richard N. Zare†

Gamma-aminobutyrate acid, L-glutamate, and *N*-methyl-D-aspartate were separated by capillary electrophoresis and detected by the use of whole-cell and outside-out patch-clamp techniques on freshly dissociated rat olfactory interneurons. These neuroactive compounds could be identified from their electrophoretic migration times, unitary channel conductances, and power spectra that yielded corner frequencies and mean single-channel conductances characteristic for each of the different agonist-receptor interactions. This technique has the sensitivity to observe the opening of a single ion channel for agonists separated by capillary electrophoresis.

We describe here a general method for the separation and detection of compounds that trigger the opening of ligand-gated ion channels. In addition to detecting established neurotransmitters and hormones, this method can be helpful for discovering bioactive substances and for identifying excitotoxins that promote receptor-mediated neurotoxicity. We applied this method to identify, from a three-component mixture, γ-aminobutyrate acid (GABA) and Glu, the major inhibitory and excitatory neurotransmitters in the mammalian brain (*1*, *2*), and *N*-methyl-D-aspartate (NMDA), a synthetic model agonist for NMDA receptors (*3*). Like many biologically active compounds, these compounds are difficult to

---

O. Orwar, A. Moscho, H. A. Fishman, R. N. Zare, Department of Chemistry, Stanford University, Stanford, CA 94305, USA.
K. Jardemark and I. Jacobson, Department of Anatomy and Cell Biology, Göteborg University, S-413 90, Göteborg, Sweden.
R. H. Scheller, Department of Molecular and Cellular Physiology, Howard Hughes Institute, Stanford University, Stanford, CA 94305, USA.

*Present address: Astra Hässle AB, S-431 83 Mölndal, Sweden.

†To whom correspondence should be addressed.